THE JOURNAL OF BIOLOGICAL CHEMISTRY VOL. 283, NO. 1, pp. 324–331, January 4, 2008

Snapin Interacts with the Exo70 Subunit of the Exocyst and Modulates GLUT4 Trafficking*[S]

Received for publication, August 17, 2007, and in revised form, October 2, 2006 Published, JBC Papers in Press, October 18, 2007, DOI 10.1074/jbc.M706873200

Yiqun Bao[‡1], **Jamie A. Lopez**[§1], **David E. James**[§2], **and Walter Hunziker**[‡3]

From the [‡]*Epithelial Cell Biology Laboratory, Institute of Molecular and Cell Biology, 61 Biopolis Drive, Singapore 138673, Singapore and the* [§]*Diabetes and Obesity Research Program, Garvan Institute of Medical Research, 384 Victoria Street, Darlinghurst New South Wales, Sydney 2010, Australia*

The exocyst is a multisubunit complex that has been implicated in the transport of vesicles from the Golgi complex to the plasma membrane, possibly acting as a vesicle tether and contributing to the specificity of membrane fusion. Here we characterize a novel interaction between the Exo70 subunit of the exocyst and Snapin, a ubiquitous protein known to associate with at least two t-SNAREs, SNAP23 and SNAP25. The interaction between Exo70 and Snapin is mediated via an N-terminal coil-coil domain in Exo70 and a C-terminal helical region in Snapin. Exo70 competes with SNAP23 for Snapin binding, suggesting that Snapin does not provide a direct link between the exocyst and the SNARE complex but, rather, mediates cross-talk between the two complexes by sequential interactions. The insulin-regulated trafficking of GLUT4 to the plasma membrane serves to facilitate glucose uptake in adipocytes, and both SNAP23 and the exocyst have been implicated in this process. In this study, depletion of Snapin in adipocytes using RNA interference inhibits insulin-stimulated glucose uptake. Thus, Snapin interacts with the exocyst and plays a modulatory role in GLUT4 vesicle trafficking.

SNAREs[4] are central components of the vesicle docking and fusion machinery (1, 2). *In vitro* liposome fusion experiments have shown that SNAREs alone are sufficient to catalyze fusion but at a much slower rate than occurs *in vivo* (3). *In vivo*, vesicle docking and fusion likely requires additional components to tightly regulate the specificity and kinetics of membrane fusion.

The seminal work of Novick and Scheckman (4) identified several genes necessary for secretion in yeast, collectively named the *SEC* genes. Temperature-sensitive mutations in each of these genes block secretion of invertase and accumulate membrane-bound organelles within the yeast cell. Six of the *SEC* genes, *SEC3*, *SEC5*, *SEC6*, *SEC8*, *SEC10*, and *SEC15*, encode subunits of an evolutionarily conserved octameric protein complex known as the exocyst. Two additional components, Exo70p and Exo84p, were subsequently biochemically purified in complex with the exocyst proteins (5–7). Similar to their yeast homologues, the mammalian exocyst proteins have been implicated in the transport of vesicles from the Golgi to the plasma membrane (8). The exocyst complex has also been implicated in the trafficking of GLUT4 vesicles to the plasma membrane (9). Among its proposed roles, the exocyst is thought to function as a vesicle tether at the plasma membrane and contribute to the specificity of membrane fusion (5). Recent studies in the β-cell demonstrated that the exocyst regulates the ability of insulin granules to dock with the plasma membrane (10).

Within the cell, each step of membrane trafficking is coupled to maintain the sequential nature and ensure the high fidelity of the process. Emerging evidence suggests a link between the membrane tethering and the SNARE-mediated docking/fusion steps (11, 12). Genetic experiments in yeast are consistent with the SNAREs acting directly downstream of the exocyst. For example, overexpression of yeast Sec1p or the t-SNAREs Sso1p/Sso2p can bypass secretory blocks induced by mutations in the exocyst genes (13, 14). In yeast, the exocyst associates through Sec15p with the vesicle-bound Rab-GTPase Sec4p (7) and acts as an effector for Sec4p during targeting of secretory vesicles to sites of exocytosis (15). In addition, the exocyst interacts with the yeast Lgl homologue Sro7p and the t-SNARE Sec9p (16, 17). The above data highlight the involvement of multiple protein-protein interactions and the potential complexity of the coupling mechanism between tethering, docking, and fusion.

Exo70 is a central component of the mammalian exocyst complex, demonstrating specific interactions with almost all of the other subunits, including Sec5, Sec6, Sec8, Sec10, and Exo84 (18, 19). Exo70 has recently been implicated in GLUT4 trafficking through its association with the GTP-bound form of the Rho GTPase TC10 (9). Stimulation of 3T3-L1 adipocytes with insulin was shown to cause an increase in the abundance of Exo70 at the plasma membrane. Furthermore, overexpression of an Exo70 mutant that interacts with TC10 specifically inhibited insulin-stimulated appearance of HA-GLUT4-GFP molecules at the plasma membrane, with no apparent effect on the

* This work was supported in part by the Agency for Science and Technology (A*STAR), Singapore and by grants from the National Health and Medical Research Council and Diabetes Australia (to D. E. J.) and a National Health and Medical Research Council (NHMRC) Dora Lush postgraduate scholarship (to J. A. L.). The costs of publication of this article were defrayed in part by the payment of page charges. This article must therefore be hereby marked "*advertisement*" in accordance with 18 U.S.C. Section 1734 solely to indicate this fact.

[S] The on-line version of this article (available at http://www.jbc.org) contains supplemental Fig. S1.

[1] Both authors contributed equally to this work.

[2] An NHMRC Senior Principal Research Fellow. To whom correspondence may be addressed. Tel.: 02-9295-8210; Fax: 02-9295-8201; E-mail: d.james@garvan.org.au.

[3] To whom correspondence may be addressed. Tel.: 65-6586-9599; Fax: 65-6779-1117; E-mail: hunziker@imcb.a-star.edu.sg.

[4] The abbreviations used are: SNARE, soluble NSF attachment protein receptor; GFP, green fluorescent protein; HA, hemagglutinin; GLUT4, glucose transporter 4; GST, glutathione *S*-transferase; PBS, phosphate-buffered saline; siRNA, small interference RNA; MBP, maltose-binding protein.

trafficking of GLUT4 to the plasma membrane. Using RNA interference, a follow-up study showed that Exo70 is critical for insulin-regulated glucose uptake in 3T3-L1 adipocytes (20). However, in both studies, the precise mechanism of Exo70 function was not defined. More recently, Exo70 has been demonstrated to interact with the Arp2/3 complex in an epidermal growth factor-dependent manner in HeLa cells. This interaction was essential for the formation of actin-based membrane protrusions and cell migration (21). Furthermore, epidermal growth factor stimulation resulted in recruitment of Exo70 to the plasma membrane, which is consistent with the observation in adipocytes. These studies suggest that growth factor signaling regulates Exo70 function, making Exo70 an interesting candidate for hormone-regulated exocytic events.

To further investigate the functional role of Exo70 in GLUT4 trafficking, we set out to identify new Exo70 interacting proteins that may facilitate the tethering and docking of GLUT4 vesicles at the plasma membrane. Here we show that Exo70 interacts with Snapin. This observation is exciting, because Snapin has previously been shown to interact with SNAP23 (22), a major t-SNARE regulating GLUT4 vesicle trafficking (23). Furthermore, we provide evidence for a modulatory role for Snapin in GLUT4 trafficking, possibly by coordinating vesicle tethering and docking through sequential interactions with the exocyst and SNARE complexes.

EXPERIMENTAL PROCEDURES

Antibodies—Rabbit and mouse anti-Exo70 antibodies were kindly provided by Charles Yeaman (University of Iowa) and Shu C. Hsu (Rutgers University), respectively. The remaining antibodies were commercially available and included rabbit anti-SNAP23 and rabbit anti-Snapin (Synaptic System), mouse anti-Sec6 and mouse anti-Sec8 (Stressgen), rabbit anti-Myc (Santa Cruz Biotechnology, Santa Cruz, CA), mouse anti-Myc and rat anti-HA (Roche Applied Science), rabbit anti-HA (Zymed Laboratories Inc.), rabbit anti-FLAG (Sigma), rabbit anti-14-3-3, and rabbit anti-glyceraldehyde-3-phosphate dehydrogenase (Abcam). Anti-FLAG M2-agarose was also from Sigma.

Cell Culture—COS1, 293T, and NIH3T3 cells were maintained in Dulbecco's modified Eagle's medium supplemented with 4500 mg/liter glucose, penicillin, streptomycin, and 10% fetal bovine serum. Plasmids were transfected using LipofectAMINE 2000 (Invitrogen). Human embryonic kidney (HEK) 293FT cells were purchased from Invitrogen, and 3T3-L1 murine fibroblasts were from the American Type Culture Collection (ATCC, Manassas, VA).

Yeast Two-hybrid Screen—Full-length rat Exo70 fused to the Gal4 DNA-binding domain in the pGBKT7 vector was a kind gift from Dr. Hugo Matern (Genentech, Inc.) and used as a bait to screen a mouse embryo Matchmaker cDNA library (Clontech). The mated yeast cells were selected on SD minimal medium supplemented with appropriate autotrophic factors except for adenine, histidine, leucine, and tryptophan (QDO plates), and putative positive clones grown on QDO were assayed for LacZ activity according to the protocol provided with the Matchmaker kit (Clontech). Plasmids from LacZ activity-positive clones were extracted and sequenced. The interaction of these clones was then further confirmed by individually retransforming them back into *Saccharomyces cerevisiae* stain AH109 with rat Exo70 in pGBKT7 and selected as described above and subjected to a β-galactosidase assay according to the manufacturer's protocol (Clontech).

DNA Constructs—Snapin and its deletion mutants (Snapin Δ1–12, Δ1–83, Δ120–136, Δ84–136, and Δ84–118) were cloned into either the pXJ40Myc (BamHI/XhoI) or the pXJ40FLAG (HindIII/XhoI) vector using standard recombinant DNA techniques. Snapin was cloned into the EcoRI/XhoI sites of pET-28a to generate a His-tagged construct. Exo70 and its deletion mutants (Exo70 Δ384–653, Δ1–383, Δ100–384, and Δ100–653) were cloned into the mammalian expression vector pDHAneo or the bacterial expression vector pGEX-4T-1 (EcoRI/XhoI). Exo70 constructs with a C-terminal HA tag were cloned into pcDNA. The pRRL-PGK lentiviral expression vector was obtained from R. Hoeben (Leiden University Medical Center), and the packaging vectors pMDLg/pRRE (encoding gag/pol), pRSV-Rev (encoding rev), and pMD2.G (encoding VSV-G) were obtained from D. Trono (Ecole Polytechnique Fédérale de Lausanne). The Gateway-compatible lentiviral destination vector pDEST/pRRL-PGK was constructed by subcloning the Gateway Reading Frame Cassette B (Invitrogen) into a unique HpaI site in the multiple cloning site of pRRL-PGK. Various Myc-Snapin deletions in pDEST/pRRL-PGK were obtained by first cloning into the Gateway entry vector MCS-pDONR221 (Invitrogen) followed by recombination into pDEST/pRRL-PGK using the Gateway LR clonase Enzyme Mix (Invitrogen). Plasmids were transformed into One Shot Stbl3 chemically competent cells (Invitrogen). The sequence of all cDNA constructs was verified.

In Vivo Binding Assays—Appropriate combinations of plasmids were transfected into 293T or COS1 cells using Lipofectamine 2000 (Invitrogen). Cells were lysed 24 h after transfection in lysis buffer (50 mM Tris, pH 7.5, 140 mM NaCl, 0.1% Triton X-100, 0.1% bovine serum albumin) for 30 min at 4 °C. Lysates were spun at 13,000 rpm for 20 min in a microcentrifuge, and the supernatants were then pre-cleared for 1 h with either protein A- or protein G-agarose beads. For immunoprecipitation of Myc- or HA-tagged proteins, the precleared lysates (500 μg of protein) were incubated overnight with rabbit anti-Myc or rat anti-HA and then captured by protein A or protein G-agarose beads for 2 h. Total rabbit or mouse IgG served as a control. For immunoprecipitation of FLAG-tagged proteins, precleared lysates were incubated with monoclonal M2 anti-FLAG beads for 2 h. Beads were then washed 5 times with lysis buffer.

In Vitro Binding Assays—For GST pulldown experiments, 10 μg each of GST, Exo70-GST, or Exo70 Δ100–653-GST were first incubated with glutathione Sepharose-4B beads (PerkinElmer Life Sciences) in GST binding buffer (50 mM Tris, pH 7.5, 1 mM $MgCl_2$, 1 mM dithiothreitol) for 1 h and then washed with GST binding buffer supplemented with 0.5% Nonidet P-40 twice. 10 μg of His-Snapin in lysis buffer was then added to each tube. After 2-h incubation, the beads were washed 4 times in lysis buffer and twice in lysis buffer supplemented with 0.5% Triton X-100. For the *in vitro* competition assays, 250 nM MBP-SNAP23 was first bound to amylose beads

(Biolabs) in lysis buffer for 1 h. 500 nM His-Snapin was then added together with increasing amounts either of GST, GST-Exo70, or Exo70 (cleaved from GST using a thrombin digestion kit, Novagen). After a 3-h incubation, the amylose beads were washed four times, and bound proteins were solubilized in SDS sample buffer and analyzed by SDS-PAGE and Western blot analysis. Samples were kept a 4 °C during the manipulations, and buffers were supplemented with protease inhibitors (Roche Applied Science).

Cellular Fractionation—Fractionation of adipocytes was carried out as described (24).

Confocal Microscopy—Immunofluorescence microscopy was performed on COS1 cells or lentivirus transduced 3T3-L1 adipocytes seeded on glass coverslips. Adipocytes were serum-starved for 2 h in Dulbecco's modified Eagle's medium at 37 °C and 5% CO_2 and incubated in the absence or presence of 1 or 100 nM insulin for 20 min. Cells were then washed three times in cold PBS, fixed with 3% (v/v) paraformaldehyde in PBS, blocked in 2% (w/v) bovine serum albumin containing 0.1% (w/v) saponin in PBS, and labeled with rabbit anti-Snapin and mouse monoclonal anti-Myc antibodies. Cells were subsequently labeled with appropriate Alexa-labeled antibodies. COS1 cells were fixed 24 h after transfection and labeled with monoclonal anti-Myc or Rabbit anti-HA antibody and appropriate secondary antibodies. Coverslips were mounted onto glass coverslides using Immuno-fluore mounting medium (ICN Biomedicals Inc.). Images were acquired and analyzed using a Leica laser scanning confocal microscope and software (Leica Microsystems, Wetzlar, Germany).

Lentivirus Production and Transduction of 3T3-L1 Adipocytes—Concentrated Myc-Snapin and GFP control lentivirus stocks were prepared as previously described (25, 26). Briefly, HEK-293FT cells were transfected at 70–90% confluency using calcium phosphate (26). One T150 flask was transfected with 26 μg of expression vector, 17.4 μg of pMDLg/pRRE (gag/pol) vector, 13.2 μg of pRSV-Rev (rev) vector, and 9.2 μg of pMD2.G (VSV-G) vector in 20 ml of culture medium. At 5–6 h post-transfection, medium was replaced with 12 ml of medium containing 6 mM butyric acid. Lentivirus was harvested at 24 h post-transfection. Supernatants containing the virus were collected, cleared by centrifugation (1,620 × *g*; 10 min), and concentrated using Amicon Ultracel concentration tubes (Millipore, MA). For confocal microscopy and immunoblotting, 3T3-L1 adipocytes grown in 24-well plates and at day 6 of differentiation were incubated for 24 h with 200 μl of 10-fold concentrated GFP or Snapin lentivirus containing 4 μg/ml Polybrene. After 24 h, the medium was replaced with 1 ml of culture medium. Experiments were performed at 5 days post-transduction.

siRNA-mediated Gene Silencing—Snapin siRNAs at a final concentration of 10 nM were transfected into mouse NIH3T3 cells with Lipofectamine RNAiMax reagent (Invitrogen), and cells were analyzed 48 h post-transfection. For electroporation of selected siRNAs, 3T3-L1 adipocytes at day 5 of differentiation were electroporated with either 20 nmol of control non-targeting siRNA or Snapin siRNA. Briefly, three 10-cm dishes of adipocytes were trypsinized and washed twice in PBS by resuspension and centrifugation at 200 × *g* for 5 min. Cells were resuspended in 1 ml of PBS, and this was divided between two 0.4-cm cuvettes (Bio-Rad) containing either control or Snapin siRNAs. Cells were electroporated by delivery of one 200 V/cm, 10-ms pulse using an ECM-830 electroporator (BTX Technologies, Inc., Holliston, MA). Cells were then transferred to gelatin-coated 12-well plates. At 72 h post electroporation, glucose uptake was measured, and cell lysates were prepared for Western blot analysis using rabbit anti-Snapin and as a control, rabbit anti-14-3-3 antibodies.

Glucose Uptake Assays—2-[^{3}H]Deoxyglucose uptake was measured in 12-well plates using siRNA-electroporated 3T3-L1 adipocytes as previously described (27).

RESULTS

Identification of Snapin as an Exo70-binding Protein—To identify new effectors of the exocyst subunit Exo70, a yeast two-hybrid screen of a mouse embryo cDNA library was performed using full-length rat Exo70 as bait. This screen identified 37 positive clones. Seven of these cDNA clones represented full-length mouse Snapin (accession number AF086838). The interaction between rat Exo70 and mouse Snapin in the yeast two-hybrid system was confirmed by the detection of *X*-α-galactosidase or β-galactosidase activity in plate (data not shown) or liquid (Fig. 1*A*) assays, respectively.

Snapin Associates with the Exocyst Complex in Vivo—To confirm the yeast two-hybrid results and characterize the association between Snapin with Exo70 *in vivo*, HEK cells were transfected with Myc-tagged Snapin and HA-tagged Exo70, and their association was analyzed in coimmunoprecipitation experiments. Immunoprecipitations with Myc antibody but not with control IgG pulled down HA-Exo70 (Fig. 1*C*). Likewise, Myc-Snapin was present in Exo70-HA immunoprecipitates.

To explore the association of Snapin with endogenous Exo70, overexpressed Myc-Snapin was immunoprecipitated and bound endogenous Exo70 detected using anti-Exo70 antibodies. In addition to endogenous Exo70, at least two other components of the exocyst complex, Sec6 and Sec8, were coprecipitated with Myc-Snapin (Fig. 1*B*). The presence of other exocyst subunits in the precipitated complex was not analyzed, because antibodies to these other exocyst components were not readily available.

To further confirm the association between Snapin and Exo70 established above, we analyzed the colocalization of Myc-Snapin and HA-Exo70 overexpressed in COS-1 cells by confocal microscopy. As shown in Fig. 1*D*, there was substantial colocalization between Myc-Snapin and HA-Exo70 in the perinuclear region of the cells as well as in punctate structures near the plasma membrane of cellular protrusions. Collectively, these experiments demonstrate an association of Snapin with the exocyst complex by a direct interaction with the Exo70 subunit.

Exo70 Interacts with a Helical Domain in the C Terminus of Snapin—Snapin contains an N-terminal hydrophobic domain (amino acids 1–20) and two helical domains (amino acids 37–65 and 83–119), the second of which is the major binding site for SNAP23 (22). To map the Exo70 binding domain in Snapin, a series of FLAG-Snapin truncation mutants were generated (Fig. 2*A*). These constructs were then coexpressed with

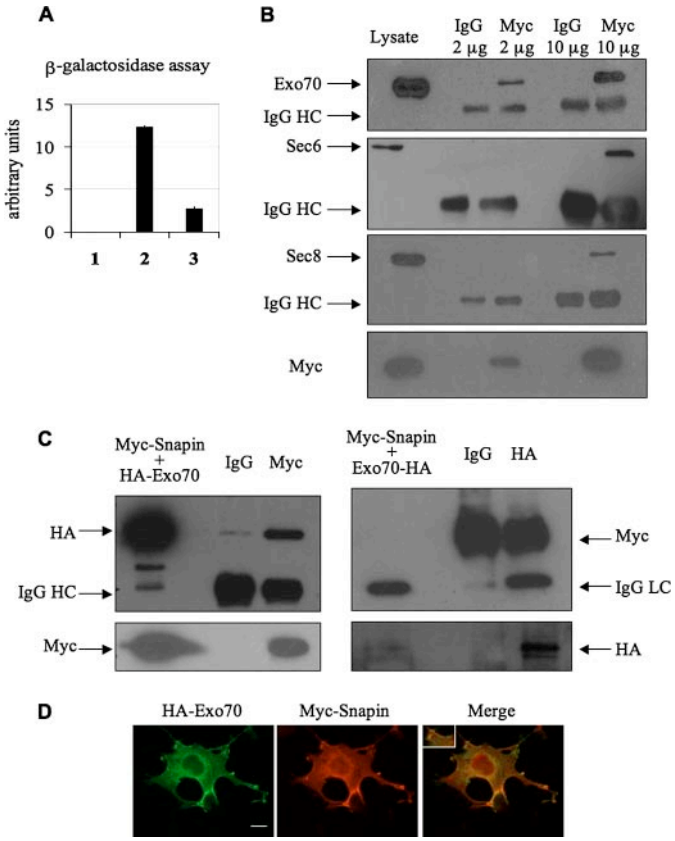

FIGURE 1. **Snapin interacts with Exo70.** *A*, yeast-two hybrid β-galactosidase assay. Liquid culture β-galactosidase assay using yeast carrying pGADT7+pGBKT7 (negative control; *bar 1*), pGADT7-T+pGBKT7-p53 (positive control; *bar 2*), and pGADT7-Snapin+pGBKT7-Exo70 (*bar 3*) were carried out using *o*-nitrophenyl-β-D-galactopyranoside as a substrate. Absorbance at 600 nm is shown in arbitrary units ($n = 3$); *error bars*, ±S.D. *B*, Myc-Snapin coprecipitates with endogenous exocyst components. Equal protein amounts of Myc-Snapin-transfected 293T cell lysates were immunoprecipitated with 2 or 10 μg of rabbit IgG (control) or rabbit anti-Myc antibodies, and immunoprecipitated proteins were analyzed by SDS-PAGE and Western blot analysis using antibodies to endogenous Exo70, Sec6, Sec8, and a mouse anti-Myc antibody. As a control, total cell lysate (50 μg) was also probed. IgG heavy chains from the antibodies used to immunoprecipitate were also detected and are indicated. *C*, Myc-Snapin and HA-tagged Exo70 interact *in vivo*. Lysates of cells coexpressing Myc-Snapin and HA-Exo70 (*left panel*) or Myc-Snapin and Exo70-HA were immunoprecipitated and bound HA-tagged Exo70 or Myc-Snapin, respectively, detected by Western blot analysis. Rabbit or rat IgG served as a control and total cell lysate was analyzed to monitor expression of the different proteins. Note that when immunoprecipitated with anti-HA antibodies, the antibodies bound to the N-terminal HA tag interfered with the association of HA-Exo70 with Myc-Snapin. *D*, Myc-Snapin and HA-Exo70 colocalize in COS1 cells. COS1 cells coexpressing Myc-Snapin and HA-Exo70 were detected by immunolabeling using mouse anti-Myc and rabbit anti-HA antibodies, followed by fluorescently labeled secondary goat antibodies and visualized using confocal microscopy. *Yellow labeling* in the merged image indicates colocalization. *Bar* = 5 μm.

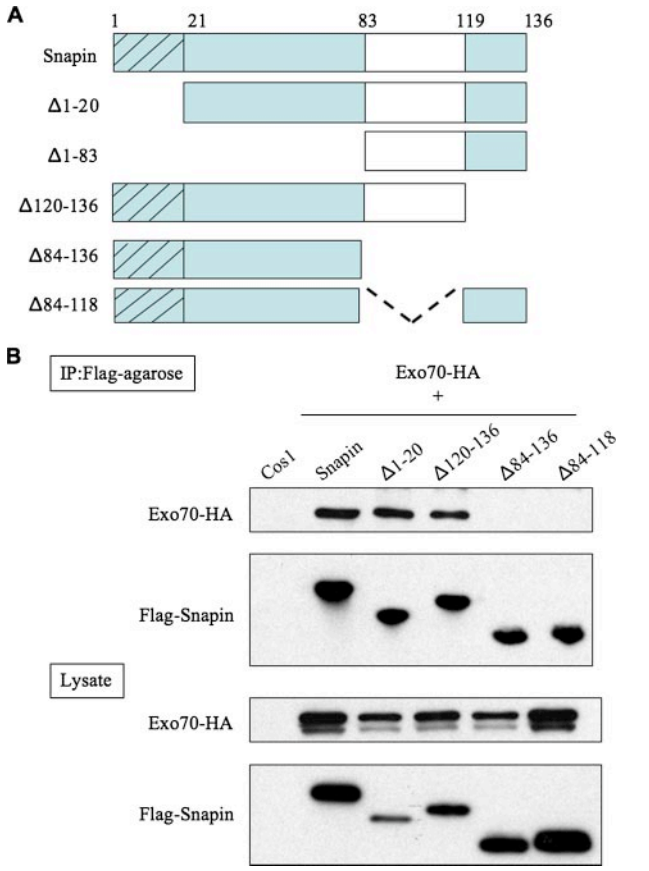

FIGURE 2. **A coil-coil domain in Snapin mediates the interaction with Exo70.** *A*, schematic diagram of mouse Snapin and its deletion mutants. Molecular modeling predicted the N-terminal first 20 amino acids to from a hydrophobic domain and residues 84–118 to form a coil-coil domain. *B*, coimmunoprecipitation of Snapin and its deletion mutants with Exo70. Lysates of COS1 coexpressing Exo70-HA and the indicated FLAG-tagged Snapin constructs were immunoprecipitated with M2 anti-FLAG beads, and the precipitates were analyzed by Western blot using anti-HA antibodies to detect bound Exo-70 or anti-FLAG antibodies to confirm binding of the FLAG-Snapin protein to the M2 beads. Cell lysates were probed with the two antibodies to monitor expression levels. Untransfected COS1 cells served as a control. The data indicate that the coil-coil domain of Snapin (amino acids 84–118) is required for binding to Exo70.

Exo70-HA in COS-1 cells, and their interaction was monitored in coimmunoprecipitation experiments. As shown above for Myc-Snapin, FLAG-Snapin robustly interacted with Exo70-HA (Fig. 2*B*). N-terminal (FLAG-Snapin Δ1–21) or C-terminal (FLAG-Snapin Δ120–136) deletions in Snapin did not affect binding to Exo70. A mutant containing only the C terminus (FLAG-Snapin Δ1–83) could not be detected by immunoblotting probably due to instability of the truncated protein (data not shown and Ref. 22). Individual deletion of either the second helical domain (FLAG-Snapin Δ84–118) or the C terminus (FLAG-Snapin Δ84–136) revealed that the presence of the second helical domain is critical for binding to Exo70. Thus, the Exo70 binding domain in Snapin maps to the second helical domain and interestingly overlaps with the SNAP23 binding site (22).

Snapin Interacts with an N-terminal Coiled-coil Domain in Exo70—To delineate the Snapin binding domain in Exo70, a series of HA-Exo70 truncation mutants were generated (Fig. 3*A*) and coexpressed with FLAG-Snapin in COS1 cells for use in coimmunoprecipitation experiments. As shown in Fig. 3*B*, Snapin showed a robust interaction with the N-terminal half of Exo70 (HA-Exo70 Δ384–653), but little if any association with the C terminus (HA-Exo70 Δ1–383). Further dissection of the N-terminal half of Exo70 revealed an interaction exclusively with amino acids 1–99 (HA-Exo70 Δ100–653) and not 100–384 (HA-Exo70 Δ100–385) (Fig. 3*B*).

The ability of the N terminus of Exo70 to directly interact with Snapin was confirmed *in vitro* using pulldown experiments with GST-Exo70 fusion proteins and purified His-tagged Snapin. There was a significant interaction between GST-

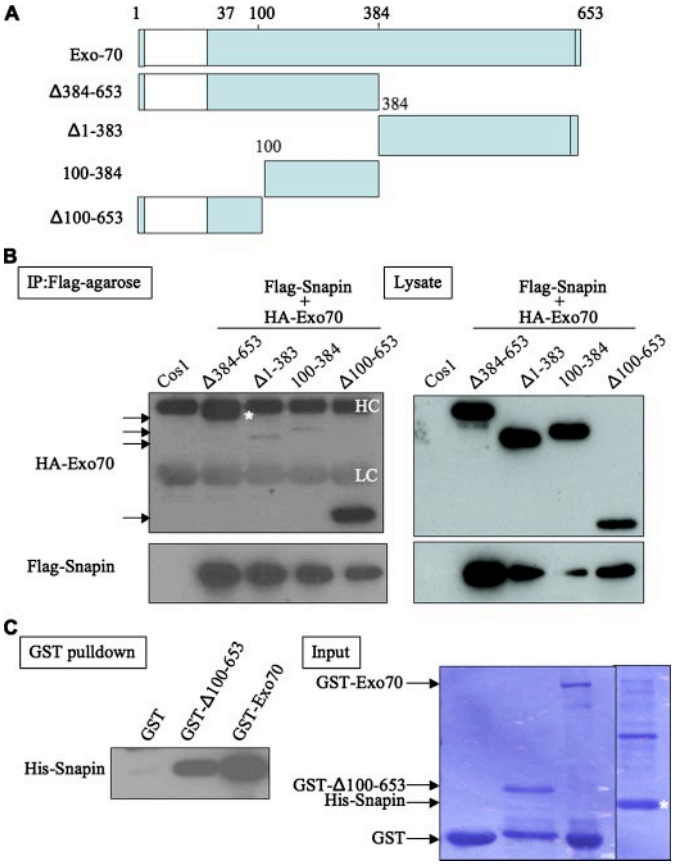

FIGURE 3. **A coil-coil domain of Exo70 mediates the interaction with Snapin.** *A*, schematic diagram of rat Exo70 and its deletion mutants. The N-terminal amino acids 5–36 form a coil-coil domain. *B*, coimmunoprecipitation of Exo70 and its deletion mutants with Snapin. Lysates of COS1 coexpressing FLAG-Snapin and the indicated HA-tagged Exo70 constructs were immunoprecipitated with M2 anti-FLAG beads, and the precipitates were analyzed by Western blot using anti-HA antibodies to detect bound HA-Exo70 or deletions, or anti-FLAG antibodies to confirm binding of the FLAG-Snapin to the M2 beads. Cell lysates were probed with the two antibodies to monitor expression levels. Untransfected COS1 cells served as a control. An *asterisk* shows the position of the Exo70 Δ385–653 band. The IgG heavy (*HC*) and light chains (*LC*) are labeled. The data show that the N terminus of Exo70, including the coil-coil domain (amino acids 5–36), is required for binding to Snapin. *C*, GST pulldown assay to demonstrate a direct interaction between the N-terminal domain of Exo70 and Snapin. GST alone or the indicated GST-Exo-70 proteins coupled to beads were incubated with purified His-tagged Snapin. Bound Snapin was detected by Western blot using rabbit anti-Snapin antibody. Deletion of the C terminus of Exo70 (amino acids 100–653) did not abolish its binding with Snapin, confirming a direct role of the N-terminal coil-coil domain. Quantity and quality of the GST and His fusion proteins used in the assay were monitored by SDS-PAGE and Coomassie Blue staining. An *asterisk* shows the position of the His-Snapin band.

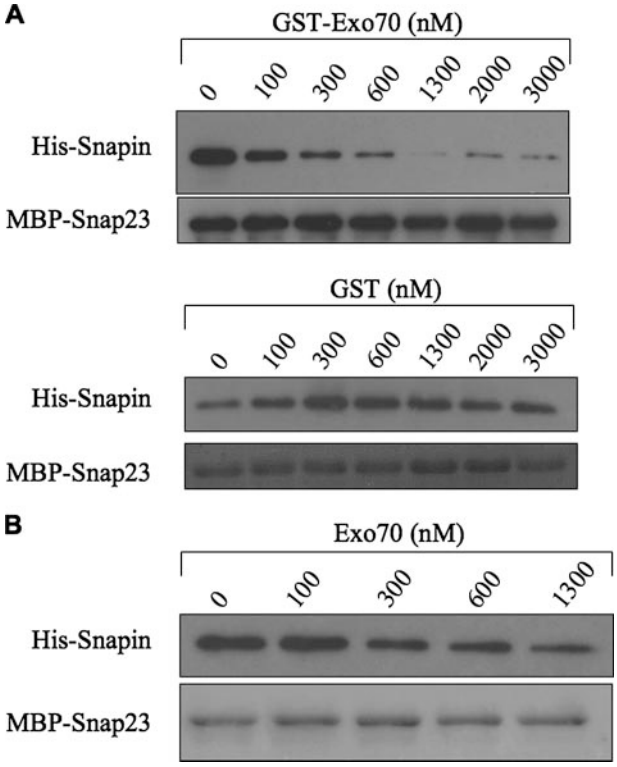

FIGURE 4. **Exo70 and SNAP23 compete for binding to Snapin.** MBP-SNAP23 (250 nM) immobilized on amylose beads was incubated with a fixed concentration of His-Snapin (500 nM) together with increasing concentrations of either GST-Exo70, GST (*A*) or Exo70 cleaved from GST (*B*). Snapin bound to the MBP-SNAP23 beads was monitored by Western blot. As a control, the amount of MBP-SNAP23 present in each reaction was also determined. The amount of His-Snapin associated with MBP-SNAP23 decreased with increasing concentrations of GST-Exo70 or Exo70, suggesting that Snapin and Exo70 compete for binding to SNAP23.

Exo70 and His-Snapin (Fig. 3*C*), whereas no binding of His-Snapin was observed using GST alone. The GST-Exo70 Δ100–653 truncation mutant interacted with His-Snapin with a similar efficiency as full-length Exo70, confirming the importance of the N terminus of Exo70 for the interaction.

These experiments confirm a direct interaction between Snapin and Exo70 and map the interaction domain in Exo70 to the N-terminal 99 residues. Interestingly, computational modeling of the Exo70 amino acid sequence revealed a putative coiled-coil domain within this region of the Exo70 N terminus.

Exo70 and SNAP23 Compete for Binding to Snapin—Because Exo70 and SNAP23 apparently interact with an overlapping region in Snapin (see above, supplemental data, and Ref. 22), we determined if Exo70 and SNAP23 simultaneously bind to Snapin, or if their association with Snapin is mutually exclusive. For this purpose, equal amounts of MBP-SNAP23 immobilized on amylose beads were incubated with His-Snapin in the presence of increasing concentrations of GST-Exo70, GST alone, or Exo70 cleaved from the GST moiety. As shown in Fig. 4 (*A* and *B*), the interaction between Snapin and SNAP23 was significantly reduced in the presence of increasing concentrations of either GST-Exo70 or cleaved Exo70 but not GST alone. We have been unable to detect any significant interaction between Exo70 and SNAP23 (data not shown), consistent with the notion that Exo70 and SNAP23 compete for the same binding site in Snapin.

Subcellular Distribution of Snapin—The Snapin-binding proteins Exo70 and SNAP23 have been shown to play a role in the final stages of GLUT4 trafficking (9, 28). Snapin itself has been previously implicated in regulated exocytic events such as calcium-induced neurosecretion (29, 30). To investigate the functional role of Snapin in vesicle docking/fusion we next studied the role of Snapin in GLUT4 trafficking in adipocytes.

Snapin was readily detected in 3T3-L1 adipocytes (Fig. 5*B*) and was predominantly targeted to the plasma membrane (Fig. 5, *A* and *B*). In contrast to SNAP23, but similar to Exo70, Snapin was present in both low and high density membrane fractions (Fig. 5*A*) in adipocytes. Stimulation of 3T3-L1 adipocytes with

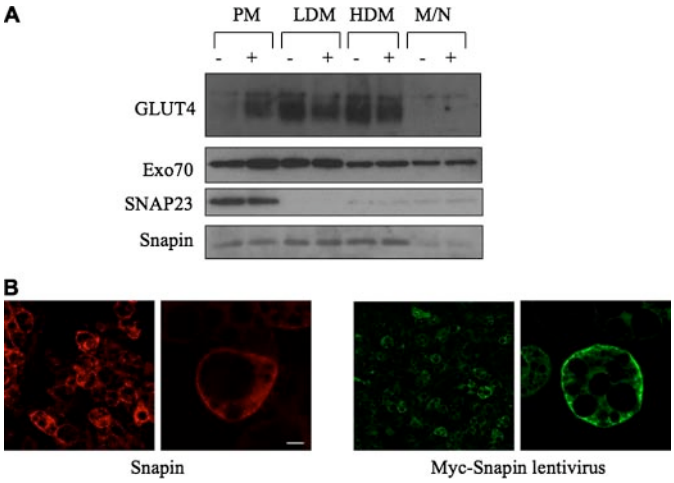

FIGURE 5. **Snapin and Exo70 localization and distribution in 3T3-L1 adipocytes.** *A*, subcellular distribution of GLTU4, Exo70, SNAP23, and Snapin. Differentiated 3T3-L1 adipocytes, either stimulated or not with 100 nM insulin for 30 min, were fractionated by differential centrifugation to obtain plasma membrane (*PM*), low density microsomes (*LDM*), high density microsomes (*HDM*), and mitochondria/nuclei (*M/N*) fractions. The presence of Glut4, Exo70, SNAP23, and Snapin in the different fractions was monitored by SDS-PAGE (10 μg of total protein for Exo70, Snapin, SNAP23; 2 μg of total protein for GLUT4) and Western blot. *B*, immunofluorescence localization of endogenous Snapin and lentivirus overexpressed Myc-Snapin. Differentiated 3T3-L1 adipocytes were labeled with antibodies to Snapin and Myc, and the localization of the proteins was visualized by confocal microscopy. Snapin is present on the plasma membrane and possibly vesicular structures and the cytosol. Cells transduced with a control lentivirus showed no labeling. *Bar* = 2 μm.

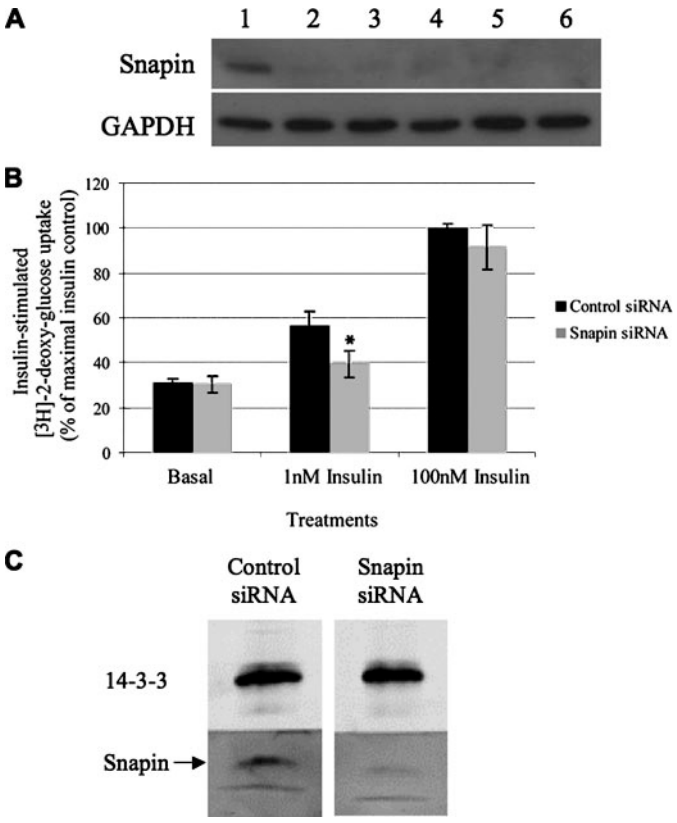

FIGURE 6. **Silencing of Snapin inhibits glucose uptake at submaximal insulin stimulation of 3T3-L1 adipocytes.** *A*, identification of effective Snapin siRNAs. Snapin expression in NIH3T3 cells (*lane 1*) was monitored by Western blot 48 h after transfection with several Snapin siRNAs. *Lanes 2–5*, 50 nM Snapin siRNA #1, #2, #3, or #4, respectively; *lane 6*, 12.5 nM of each of the four siRNAs combined. All Snapin siRNAs, alone or in combination, efficiently silenced Snapin without affecting, as a control, glyceraldehyde-3-phosphate dehydrogenase expression levels. *B*, snapin siRNA inhibits 2-deoxyglucose uptake at submaximal insulin stimulation. The Snapin siRNA pool was electroporated into differentiated 3T3-L1 adipocytes, and 72 h later the cells were treated or not with 1 nM or 100 nM insulin and 2-[^{3}H]deoxyglucose uptake was measured. Basal uptake was independent of insulin stimulation and unaffected by siRNAs. Submaximal stimulation (1 nM insulin) increased 2-deoxyglucose uptake by ~2-fold, and this was significantly inhibited by the Snapin siRNAs as compared with a control siRNA. The inhibitory effect was no longer significant at maximal insulin stimulation (100 nM; $n = 3$); *error bars*, ±S.E. *C*, silencing of Snapin in differentiated 3T3-L1 adipocytes. In parallel to the 2-deoxyglucose uptake experiment, one set of cells treated with control or Snapin siRNA was used to monitor Snapin expression by Western blot. In differentiated adipocytes, Snapin was silenced to a similar extent as in NIH3T3 cells, but the specific siRNA did not affect expression of 14-3-3, which served as a control.

insulin, which results in the translocation of GLUT4 to the plasma membrane (Fig. 5*A*), did not affect the subcellular distribution of Snapin. As previously reported for the exocyst (9), an enrichment of Exo70 in the plasma membrane fraction was observed after insulin stimulation of 3T3-L1 adipocytes.

Snapin Modulates Insulin-stimulated GLUT4 Trafficking—To explore a possible functional role for Snapin in insulin-regulated GLUT4 vesicle trafficking, we next studied the effect of modulating Snapin expression on insulin action in adipocytes. 3T3-L1 adipocytes were infected with lentivirus expressing full-length Myc-Snapin. Despite some variability in Snapin expression between individual cells, immunofluorescence microscopy revealed that >90% of the cells in the culture were expressing Myc-Snapin. Moreover, immunoblotting revealed a protein product of the expected size for Myc-Snapin in adipocytes (data not shown). The localization of Myc-Snapin was indistinguishable from the endogenous protein indicating that the protein was not vastly overexpressed using this approach (Fig. 5*B*). Cells overexpressing Myc-Snapin did not exhibit any impairment in insulin-stimulated glucose transport (data not shown). We also expressed a range of Snapin mutants in adipocytes using this same approach, but again we were unable to detect any impairment in insulin action (data not shown).

We next examined the effects of reduced Snapin expression on insulin action using RNA interference. As shown in Fig. 6*A*, we identified four different siRNAs that efficiently reduced Snapin protein levels when transfected either individually or as a pool into either NIH3T3 or 3T3-L1 cells. The expression of control proteins, either glyceraldehyde-3-phosphate dehydrogenase or 14-3-3 was unaffected under these conditions. As shown in Fig. 6*B*, reduced Snapin expression had no effect on 2-deoxyglucose uptake in either the absence of insulin or in the presence of a maximum dose of insulin. However, at submaximal concentrations of insulin, where we observed an ~2-fold effect of insulin on 2-deoxyglucose uptake in control cells, reduced Snapin expression resulted in a blunted response. These observations implicate a role for Snapin in insulin-stimulated glucose transport in adipocytes likely by modulating the tethering or docking/fusion of GLUT4 containing vesicles with the plasma membrane.

DISCUSSION

Snapin was originally identified in a human brain yeast two-hybrid screen as an SNAP25 interacting protein (29). This initial study suggested Snapin was a neuronal-specific protein,

because a Snapin-specific antibody was unable to detect Snapin in other tissues. It was later demonstrated by Northern blotting and subsequent Western blotting, that Snapin is ubiquitously expressed and in fact also can bind the SNAP25 homologue SNAP23 (22). However, the latter study did not address the functional significance of the SNAP23 and Snapin interaction.

In the present studies, Snapin was identified in a yeast two-hybrid screen as an Exo70-binding protein. Snapin was shown to associate, through Exo70, with additional exocyst components, suggesting that it interacts with the native exocyst complex. Buxton and colleagues (22) have previously shown that Snapin can also form a complex with SNAP23 and Syntaxin4 *in vitro*. This finding is interesting, because Snapin may represent a prime candidate for mediating or regulating exocyst and SNARE complex interactions. Because SNAP23 and Exo70 appear to bind Snapin in the same C-terminal portion, it is interesting to speculate that crosstalk between exocyst and SNARE complexes may be transferred by sequential binding to Snapin.

In vivo binding experiments demonstrated that the Snapin interaction is mediated through the N-terminal 99 amino acids of Exo70. The crystal structure of yeast Exo70p was recently published (31), and sequence alignments suggest that the mammalian orthologues have similar structural domains. Exo70p consists of multiple helical bundles, which are divided into three domains to form an elongated structure. Interestingly, the first 99 amino acids are predominantly surface-exposed residues, which is consistent with them contributing to a protein interaction site. The N terminus of Exo70 also serves as the binding site for TC10, and overexpression of the N terminus of Exo70 (Exo70-N: amino acid 1–384) in 3T3-L1 adipocytes was shown to inhibit fusion of GLUT4 vesicles with the plasma membrane (9). The effect of this mutant is thought to be due to competitive displacement of endogenous Exo70 for TC10 binding sites. Based on our findings, an alternative explanation is that the Exo70-N mutant competes for binding of Snapin on the plasma membrane.

Experiments in chromaffin cells suggest a positive regulatory role for Snapin in exocytosis (30). This study showed that Snapin is phosphorylated by protein kinase A, resulting in its enhanced affinity for SNAP25 and an increased association of synaptotagmin with SNARE complexes. Overexpression of a phosphomimetic Snapin mutant resulted in increased exocytosis of large dense core vesicles. Earlier studies demonstrated that overexpression of the C terminus of Snapin or injection of Snapin peptides corresponding to the SNAP25 binding site have a slight inhibitory effect on synaptic transmission (29). In this study, knockdown of Snapin caused a reduction in insulin-stimulated glucose transport. This effect was only observed at submaximal insulin concentrations likely, because the knockdown of endogenous Snapin was incomplete. Snapin knockout mice have recently been described (32), and consistent with our findings, Snapin was shown to have a modulatory role in neurosecretion, because the absence of Snapin resulted in significantly reduced exocytosis in embryonic chromaffin cells. We speculate that reduction of Snapin may impair the dialogue between the exocyst and SNARE complex assembly.

We did not observe any consequence of over expression of Snapin or C-terminal truncation mutants on insulin-stimulated glucose transport in adipocytes (data not shown). This may denote that these proteins were not expressed at sufficiently high levels to observe a phenotype. This interpretation is consistent with a more recent publication re-investigating the role of Snapin in neurosecretion (33). In contrast to the two prior studies, Vites and co-authors were unable to observe defects in synaptic transmission induced by Snapin mutant overexpression. The overexpression studies performed in the present studies, however, do not exclude a role for Snapin in GLUT4 trafficking, because it cannot be confirmed that overexpression of Snapin *wt* and/or mutants would have a dominant negative effect. The presence of the endogenous Snapin may be sufficient to allow normal GLUT4-trafficking events. Our data thus suggest that, although Snapin may not ultimately be required, it plays a positive role, possibly by regulating the fidelity of GLUT4 vesicle docking. Future work will elucidate the precise mechanism of action of Snapin in targeting, docking, or fusion of GLUT4 vesicles and explore the physiological role of Snapin in glucose homeostasis.

The present studies have thus identified a novel interaction of Snapin with the exocyst and a novel modulatory role for Snapin in insulin-stimulated GLUT4 vesicle transport in adipocytes.

Acknowledgments—We thank Drs. Rob Hoeben, Shu Hsu, Hugo Matern, Didier Trono, and Charles Yeaman for their kind gift of reagents.

REFERENCES

1. Hardwick, K. G., and Pelham, H. R. B. (1992) *J. Cell Biol.* **119,** 513–521
2. Shim, J., Newman, A. P., and Ferronovick, S. (1991) *J. Cell Biol.* **113,** 55–64
3. Weber, T., Zemelman, B. V., McNew, J. A., Westermann, B., Gmachl, M., Parlati, F., Sollner, T. H., and Rothman, J. E. (1998) *Cell* **92,** 759–772
4. Novick, P., Field, C., and Schekman, R. (1980) *Cell* **21,** 205–215
5. Munson, M., and Novick, P. (2006) *Nat. Struct. Mol. Biol.* **13,** 577–581
6. TerBush, D. R., Maurice, T., Roth, D., and Novick, P. (1996) *EMBO J.* **15,** 6483–6494
7. Guo, W., Grant, A., and Novick, P. (1999) *J. Biol. Chem.* **274,** 23558–23564
8. Grindstaff, K. K., Yeaman, C., Anandasabapathy, N., Hsu, S. C., Rodriguez-Boulan, E., Scheller, R. H., and Nelson, W. J. (1998) *Cell* **93,** 731–740
9. Inoue, M., Chang, L., Hwang, J., Chiang, S. H., and Saltiel, A. R. (2003) *Nature* **422,** 629–633
10. Tsuboi, T., Ravier, M. A., Xie, H., Ewart, M. A., Gould, G. W., Baldwin, S. A., and Rutter, G. A. (2005) *J. Biol. Chem.* **280,** 25565–25570
11. Conibear, E., Cleck, J. N., and Stevens, T. H. (2003) *Mol. Biol. Cell* **14,** 1610–1623
12. Stroupe, C., Collins, K. M., Fratti, R. A., and Wickner, W. (2006) *EMBO J.* **25,** 1579–1589
13. Aalto, M. K., Ronne, H., and Keranen, S. (1993) *EMBO J.* **12,** 4095–4104
14. Wiederkehr, A., De Craene, J. O., Ferro-Novick, S., and Novick, P. (2004) *J. Cell Biol.* **167,** 875–887
15. Guo, W., Roth, D., Walch-Solimena, C., and Novick, P. (1999) *EMBO J.* **18,** 1071–1080
16. Novick, P., Medkova, M., Dong, G., Hutagalung, A., Reinisch, K., and Grosshans, B. (2006) *Biochem. Soc. Trans.* **34,** 683–686
17. Sivaram, M. V. S., Saporita, J. A., Furgason, M. L. M., Boettcher, A. J., and Munson, M. (2005) *Biochemistry* (*Mosc.*) **44,** 6302–6311
18. Matern, H. T., Yeaman, C., Nelson, W. J., and Scheller, R. H. (2001) *Proc. Natl. Acad. Sci. U. S. A.* **98,** 9648–9653
19. Vega, I. E., and Hsu, S. C. (2001) *J. Neurosci.* **21,** 3839–3848
20. Inoue, M., Chiang, S. H., Chang, L., Chen, X. W., and Saltiel, A. R. (2006) *Mol. Biol. Cell* **17,** 2303–2311

21. Zuo, X. F., Zhang, J., Zhang, Y., Hsu, S. C., Zhou, D. G., and Guo, W. (2006) *Nat. Cell Biol.* **8,** 1383-U1338
22. Buxton, P., Zhang, X. M., Walsh, B., Sriratana, A., Schenberg, I., Manickam, E., and Rowe, T. (2003) *Biochem. J.* **375,** 433–440
23. Rea, S., Martin, L. B., McIntosh, S., Macaulay, S. L., Ramsdale, T., Baldini, G., and James, D. E. (1998) *J. Biol. Chem.* **273,** 18784–18792
24. Thurmond, D. C., Ceresa, B. P., Okada, S., Elmendorf, J. S., Coker, K., and Pessin, J. E. (1998) *J. Biol. Chem.* **273,** 33876–33883
25. Carlotti, F., Bazuine, M., Kekarainen, T., Seppen, J., Pognonec, P., Maassen, J. A., and Hoeben, R. C. (2004) *Mol. Ther.* **9,** 209–217
26. Li, M. J., and Rossi, J. J. (2005) *RNA Int.* **392,** 218–226
27. Malide, D., Ramm, G., Cushman, S. W., and Slot, J. W. (2000) *J. Cell Sci.* **113,** 4203–4210
28. Kawanishi, M., Tamori, Y., Okazawa, H., Araki, S., Skinoda, H., and Kasuga, M. (2000) *J. Biol. Chem.* **275,** 8240–8247
29. Ilardi, J. M., Mochida, S., and Sheng, Z. H. (1999) *Nat. Neurosci.* **2,** 119–124
30. Chheda, M. G., Ashery, U., Thakur, P., Rettig, J., and Sheng, Z. H. (2001) *Nat. Cell Biol.* **3,** 331–338
31. Hamburger, Z. A., Hamburger, A. E., West, A. P., and Weis, W. I. (2006) *J. Mol. Biol.* **356,** 9–21
32. Tian, J. H., Wu, Z. X., Unzicker, M., Lu, L., Cai, Q., Li, C. L., Schirra, C., Matti, U., Stevens, D., Deng, C. X., Rettig, J., and Sheng, Z. H. (2005) *J. Neurosci.* **25,** 10546–10555
33. Vites, O., Rhee, J. S., Schwarz, M., Rosenmund, C., and Jahn, R. (2004) *J. Biol. Chem.* **279,** 26251–26256